2011 NDIA GROUND VEHICLE SYSTEMS ENGINEERING AND TECHNOLOGY SYMPOSIUM
POWER AND MOBILITY (P&M) MINI-SYMPOSIUM
AUGUST 9-11 DEARBORN, MICHIGAN

THE CHALLENGES OF COMPARING PROPULSION COOLING CFD STUDIES TO TEST CHAMBER AND ON-ROAD PERFORMANCE

Scott Shurin
Thermal & Signature
Modeling Team
TARDEC
Warren, MI

Vamshi M. Korivi, PhD
Thermal & Signature
Modeling Team
TARDEC
Warren, MI

ABSTRACT

The thermal test chambers available at TARDEC for validation and development testing are different in terms of capability, size, and flow setup. The effects of the chamber setup on propulsion cooling airflow and the challenges of using thermal chamber tests to correlate CFD results and predict off-road performance will be discussed. Numerical simulation and test results for both a tracked combat vehicle tested in a large test cell and a wheeled MRAP vehicle tested in a smaller test cell will be presented. Numerical simulation results for these two different vehicles in on-road type of scenario and test chamber scenario at full-load cooling will be compared and contrasted. Results from CFD simulation with test cell set-up will be compared with actual physical testing in the test chamber. Procedures used for the propulsion cooling CFD simulation, best practices, limitations, and recommended procedure will be presented in detail.

INTRODUCTION

Full load cooling tests are performed in test chambers at TARDEC to determine the tractive effort, speed on grade, and maximum speed of both tracked and wheeled vehicles under different ambient temperatures. In these cells, the vehicle is stationary and the drivetrain is connected to one or more dynamometers to provide power absorption and measure the engine power and torque. The tractive capability is calculated based on the vehicle weight, tire radius, planetary gear ratio, and differential gear ratio. The velocity and temperature of the air entering the cell can be controlled by varying fan speed and steam temperature.

During tests, the vehicle under test is instrumented with various pressure transducers, thermocouples, flow meters, and tachometers to acquire data on the performance of the vehicle cooling system. Heat exchangers are typically instrumented with a thermocouple array to measure the upstream and downstream air temperatures. Oil and coolant temperatures are measured at the inlet and outlet of each heat exchanger in the system. In addition, transmission oil temperature, engine oil temperature, and sump temperatures for these fluids is also monitored. Typically the tractive effort capability is based on the ability of the cooling system to maintain the coolant top tank temperature below 230 °F and transmission oil cooler inlet temperature below 280 °F.

In this paper an attempt is made to compare propulsion cooling simulation results from vehicle tests conducted under test cell environments to off-road conditions for two vehicles. The first vehicle, a wheeled Mine Resistant Ambush Protected (MRAP) vehicle, was immersed in a relatively small cell (Cell 5). The second vehicle, a tracked vehicle, was immersed in larger cell (Cell 9).

ANALYSIS METHODOLOGY

The procedure followed for performing Computational Fluid Dynamics (CFD) simulations for each vehicle was similar. The original CAD geometry of the vehicle is tessellated and organized into different assemblies based on function (e.g. exterior surface, powertrain, fan region, heat exchanger) using pre-processing software. Special care is taken in the vicinity of the heat exchangers, fan, and heat exchanger shrouds since these components represent the main area of interest for this type of analysis. The vehicle geometry is immersed in a tunnel environment for analysis.

The heat exchangers are modeled using a porous media approach. In the porous media approach the flow restriction is modeled based on manufacturer curves of pressure drop versus velocity but the internal details of the heat exchanger are not modeled. Heat rejection characteristics are modeled using a single stream heat exchanger model and

manufacturer curves of heat rejection versus flow rate. Sample radiator performance data is shown in Figure 1.

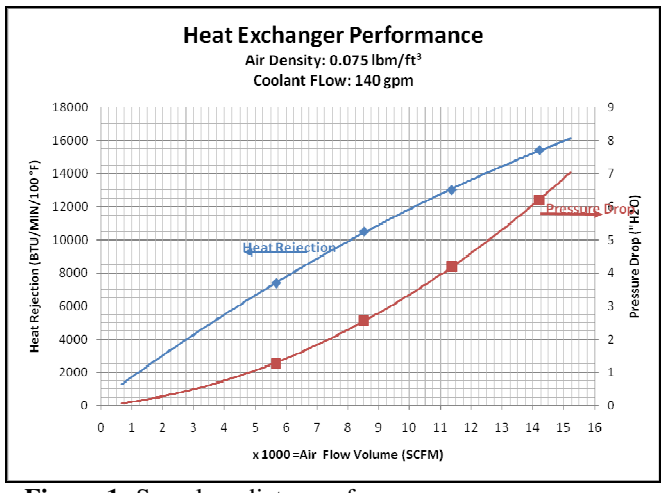

Figure 1: Sample radiator performance curves.

Another critical element of the analysis is the fan or fans. The precise fan blade geometry is typically proprietary, so a detailed model of fan cannot be used. Instead, the fan is modeled using a momentum source based on fan performance curves supplied by the manufacturer. Typically, the fan performance curve is generated based on bench testing following Air Movement and Control Association (AMCA) standards at a constant rotation rates and density. The resulting curves can be scaled to the appropriate fan inlet air density and fan rotation rate by applying the fan laws for pressure rise and flow volume.

For purposes of simulation it is more convenient to transform the fan performance curve into non-dimensional parameters known as the flow coefficient (φ) and pressure coefficient (ψ). These coefficients normalize the pressure rise (ΔP) and flow volume (Q) based on the fan speed (N), diameter (D), and density (ρ).

$$\psi = \frac{\Delta P}{\rho N^2 D^2} \qquad (1)$$

$$\phi = \frac{Q}{N D^3} \qquad (2)$$

To use the momentum source approach, a cylinder enclosing the fan swept volume is generated. Typically, the fan hub is also included as this represents a restriction to the flow. When modeling mechanically driven automotive fans, great care needs to be taken with modeling the fan disk to account for the effects of Fan Out Of Shroud (FOOS) and proximity to the engine. In addition, clearance between the blade tips and fan shroud is often not symmetric care should be taken to account for this when building the fan disk geometry.

Varying mesh resolutions are specified on each boundary region based on the specific details that need to be captured. In addition, volume refinement regions are defined around heat exchangers, wake regions, and in the neighborhood of grills. These refinements allow the local flow field near these areas to be captured accurately without increasing the mesh count globally. Local refinement using a trimmed mesh methodology is the preferred technique for computational reasons. Best practices for setting up the analysis are followed based on the document in reference [1].

Boundary conditions for the tunnel are specified as follows: the sides, roof, floor, and ceiling are specified as walls; the inlet plane is specified as a velocity inlet; and the exit plane is specified as a pressure boundary. The inlet boundary temperature is specified at the desired ambient temperature for the simulation. When simulating off-road conditions the sides and top of the domain are specified as symmetry boundaries and the ground plane is given a tangential velocity equal to the vehicle speed.

MRAP WHEELED VEHICLE SIMULATION RESULTS

The MRAP vehicle was tested in Cell 5. This test cell is relatively small compared to Cell 9 described later in this paper. The layout of Cell 5 is shown below in Figure 2 and Figure 3. In Cell 5 the air is heated up by steam-air heat exchangers, enters the cell, and then makes a ninety degree turn before hitting the vehicle. Air exits the tunnel through the rear after flowing over the vehicle. The cell inlet air temperature is controlled by taking the average of four thermocouple measurements taken about 3 feet in front of the vehicle.

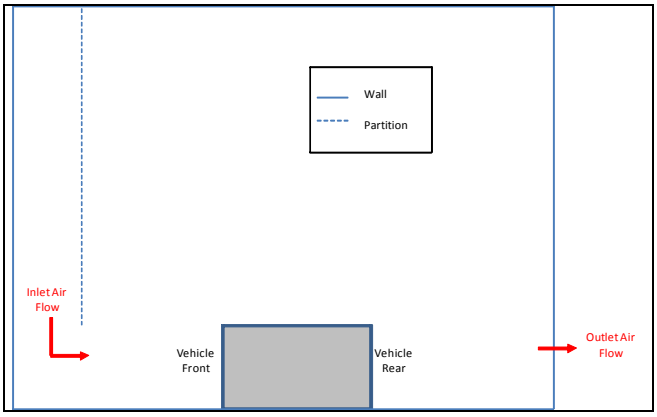

Figure 2: Side view of cell 5.

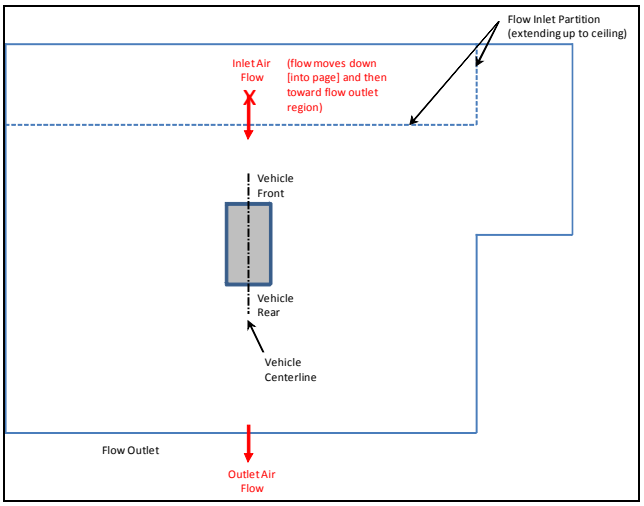

Figure 3: Top view of cell 5.

The simulation was performed at a wind speed of 5 mph and cooling fan rotation rate specified based on the operating load from the test. Simulation results are for a tractive effort of 0.6 TE/WT with the air conditions system switched off. Vendor supplied heat exchanger data was used to model the heat exchanger pressure drops and heat exchanger heat rejections. Fan performance curves were used to size the momentum source for used to represent the fan.

The layout of the condensers, charge air cooler, radiator, transmission oil cooler, and fan are shown in Figure 4. In this vehicle the air passes first through the condenser, then the charge air cooler, followed by the charge air cooler, radiator and finally the transmission oil cooler.

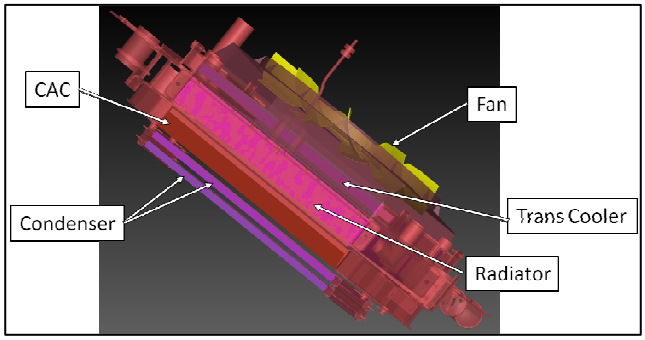

Figure 4: MRAP heat exchanger and fan layout.

The following are observations from the Cell 5 and off-road scenarios:

1. Warmer air exiting the underhood area hits the roof of the cell and recirculates back into heat exchanger as compared to the off-road condition as shown in Figure 5 and Figure 6.
2. The mass flow through the heat exchangers in Cell 5 and off-road condition is nearly identical for the tractive effort condition simulated.
3. The fan operating point for the tractive effort simulated is shown on the fan curve in Figure 7.
4. The temperature of the air entering the condenser in the Cell 5 scenario is approximately 1.8 °F hotter than the off-road scenario as shown in Figure 8 and Figure 9. However, the temperature entering the radiator for Cell 5 scenario is 2 °F cooler than in the off-road scenario as shown in Figure 10 and Figure 11.
5. As shown in Figure 12 and Figure 13, the underhood flow pattern is changed in Cell 5 as compared to the off-road condition. This is mainly attributed to the air entering perpendicular to the ground in Cell 5.
6. Predicted mass flow through the radiator from simulation and testing match within 5%.

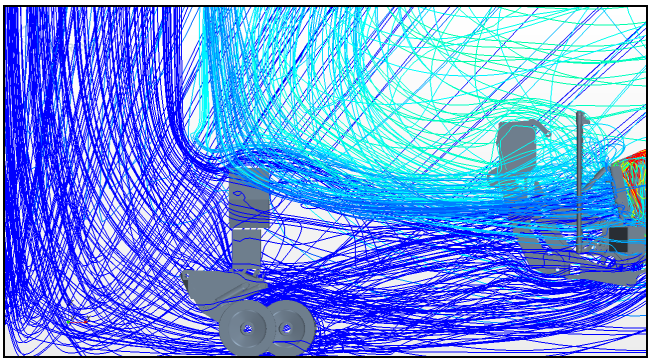

Figure 5: Streamlines colored by temperature - Cell 5.

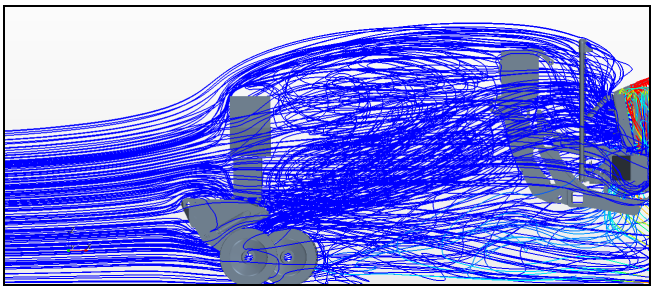

Figure 6: Streamlines colored by temperature - off-road.

For the wheeled vehicle simulated, the air flow rate was computed by using an energy balance between the engine coolant and air streams passing through the radiator. The coolant flow rate and temperature difference was used to determine the radiator heat rejection to the air. The air mass flow rate was then calculated based on heat rejection and the measured air-side temperature difference across the radiator.

The air flow rate predicted by the simulation agreed very well with the flow rate calculated using this method.

As a check, the mass flow rate was also calculated based on the heat rejection to the coolant and radiator heat rejection curve supplied by the manufacture. The air flow rate calculated using this method did not agree well with either the simulation or the flow rate calculated based on the air-side temperature difference. It is believed that for this case the supplier heat rejection curve predicted a higher heat transfer at a given air flow rate. This could be due to radiator fouling, flow non-uniformities, or an over-prediction of the radiator heat transfer performance.

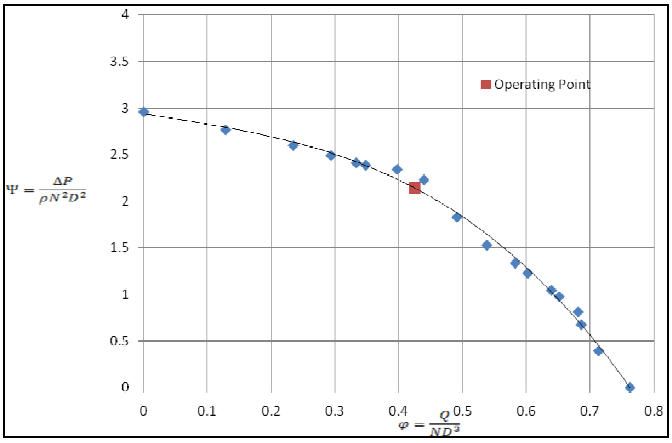

Figure 7: Fan operating point.

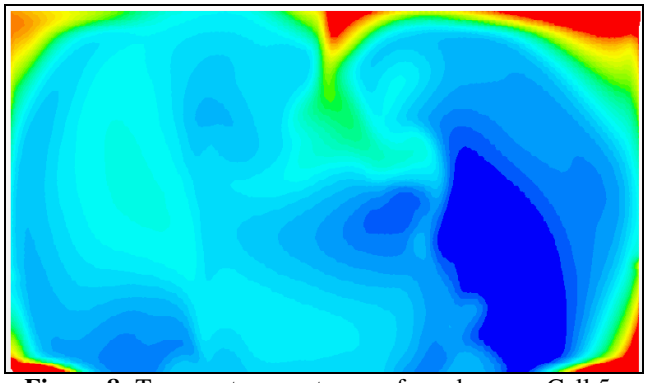

Figure 8: Temperature upstream of condenser – Cell 5.

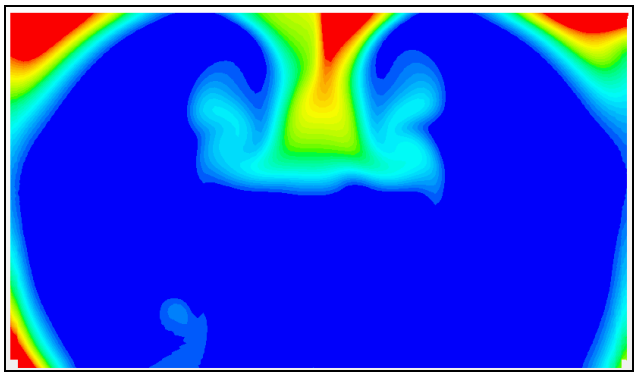

Figure 9: Temperature upstream of condenser - off-road.

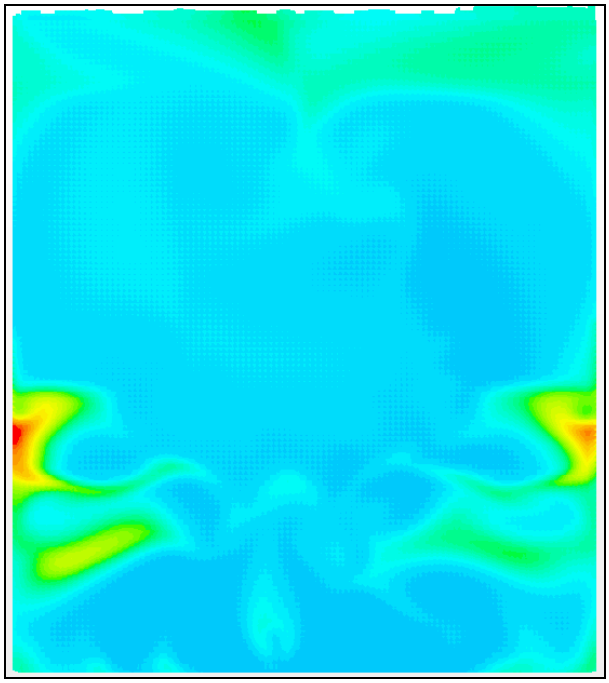

Figure 10: Temperature at radiator inlet - Cell 5.

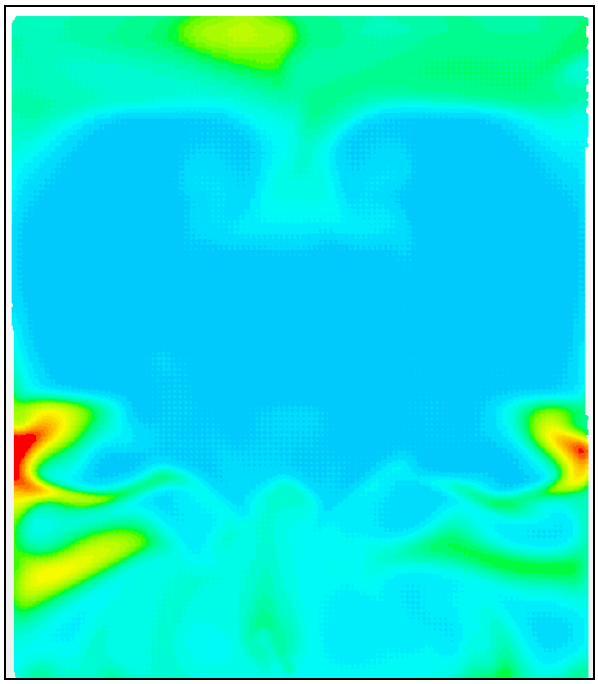

Figure 11: Temperature upstream of radiator - off-road.

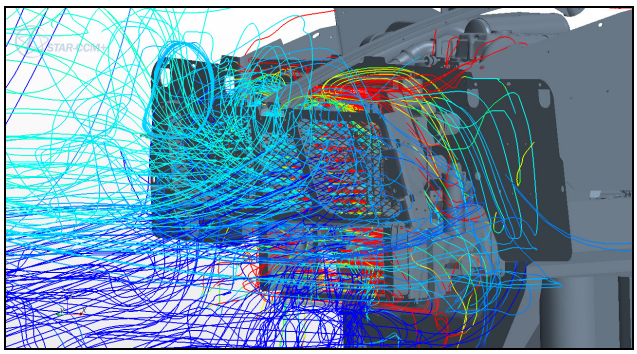

Figure 12: Streamlines entering the heat exchanger colored by temperature - Cell 5.

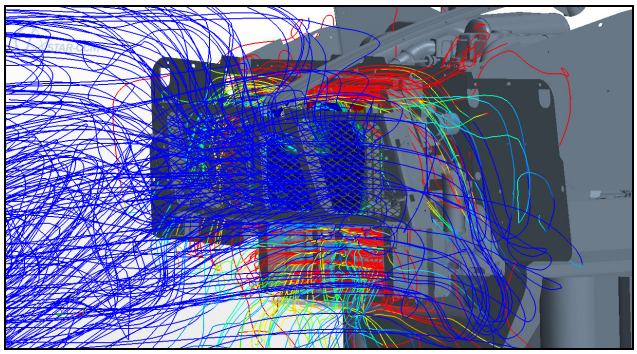

Figure 13: Streamlines entering the heat exchanger colored by temperature - off-road.

TRACKED VEHICLE SIMULATION RESULTS

The tracked vehicle was tested at TARDEC in Cell 9. A picture of a tracked vehicle undergoing testing in this cell is shown in Figure 14Figure 14. Cell 9 is cylindrical and much larger than Cell 5. The air velocity through the cell is about 4 to 5 mph. During testing a Solar Radiation Simulator light blank is placed over the engine compartment to simulate the effects of solar loading. Power from the drivetrain is absorbed through the use of two absorption dynamometers.

Figure 14: Vehicle in test cell from [2].

During testing the cell ambient temperature is controlled by measuring the air temperature at four pints located approximately 8 feet in front of the vehicle. The lower boundary of the measurement rectangle is located approximately 4 to 5 feet above the test cell floor and the upper boundary is located approximately 9 feet above the floor. It is standard practice to use the average of these four measurements to control the test cell temperature.

The primary purpose of this testing was to characterize the vehicle performance under high ambient temperatures. A secondary objective was to use the data collected during testing to verify design calculations and provide information for verifying powertrain and CFD models. Data collected included vehicle speed, fan rotation rates, air temperatures, coolant flow rates, pressures, and coolant temperatures.

During top speed testing, analysts noted that the air temperatures measured at the inlet grille were consistently higher than the wind tunnel ambient air temperature (measured at the four points mentioned previously) by about 3 to 5 °F. The purpose of the first CFD simulations was to provide an estimate of the system resistance curve. Additional simulations were used to evaluate potential explanations for the observed temperature rise.

A diagram of the analysis domain is shown in Figure 15. The approximate dimensions of Cell 9 were used to define the extents of the domain as well as the inlet and exit locations. Geometry for the vehicle cab, gun tube, and rear chassis were not available for the initial simulation. A diagram of the cooling system layout is shown in Figure 16. This vehicle has two fans located below the exit grille.

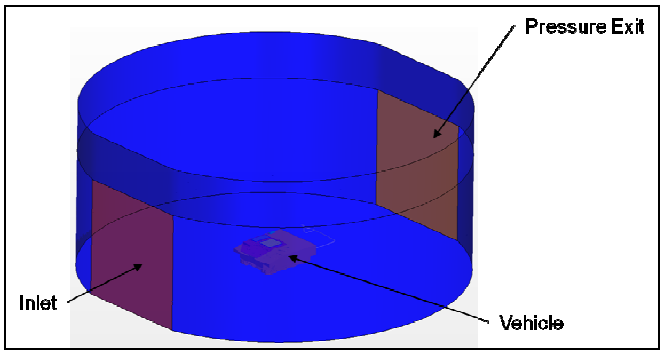

Figure 15: Analysis domain.

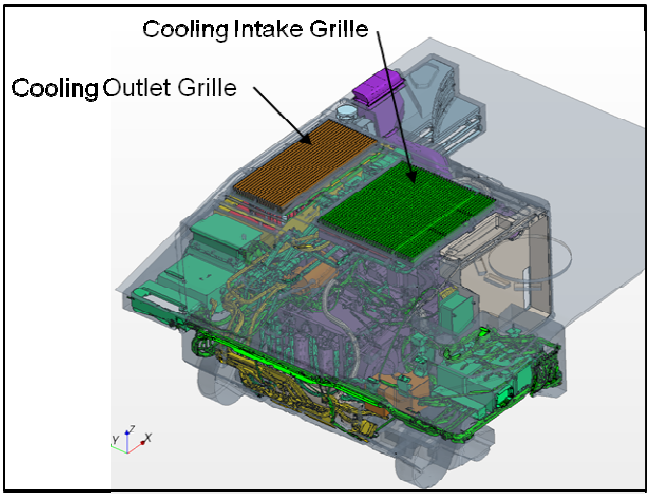

Figure 16: Vehicle geometry.

The first simulation of the vehicle in Cell 9 assumed uniform velocity and temperature at the cell inlet. The purpose of this simulation was to determine if propulsion cooling exhaust air was recirculating back into propulsion cooling inlet grille. Streamlines of the flow emanating from the fan exit are shown in Figure 17. The streamline and temperature results from the simulation indicated that the flow does not recirculate, either directly or indirectly, from the propulsion cooling exit grille into the inlet grille.

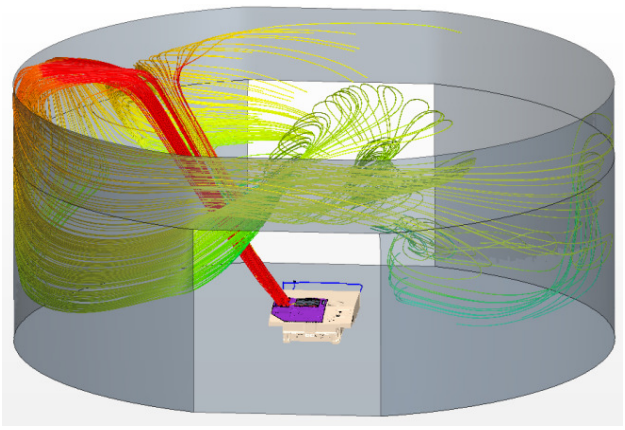

Figure 17: Streamlines colored by temperature**.**

The results from the uniform inlet simulation indicated that there was no recirculation from the propulsion cooling exhaust back into the inlet grille. An alternative explanation was that temperature stratification at the cell inlet could be causing the issue. Infrared temperature readings taken on the inlet guide vanes of the test cell indicated that there was some temperature stratification at the cell inlet. This temperature data was input into the model and a second simulation was performed. The imposed temperature field is shown in Figure 18.

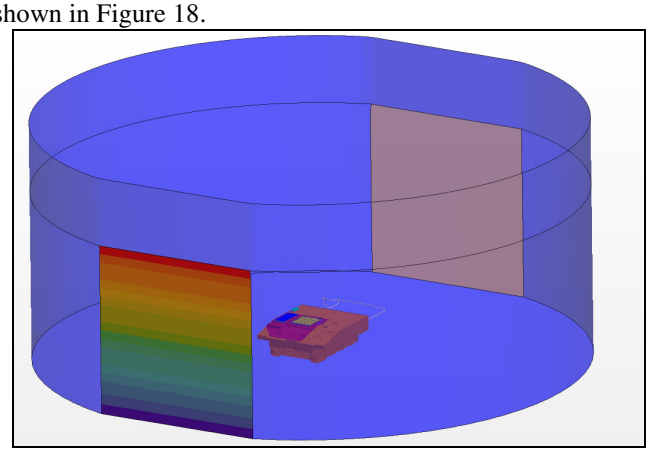

Figure 18: Inlet temperature distribution.

A plot showing the temperature contours at a plane cutting through the centerline of the vehicle is shown in Figure 19. The results show that some of the high temperature air from the upper portions of the inlet is able to enter the propulsion cooling grille. This elevates the temperature at the inlet grille to about 4 °F above the ambient cell temperature. Temperature contours at a plane just above the cooling air intake grille are shown in Figure 20.

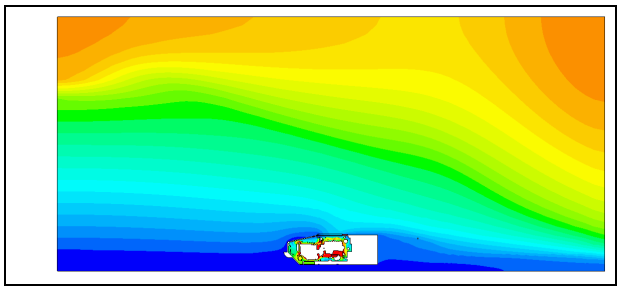

Figure 19: Temperature at vehicle centerline.

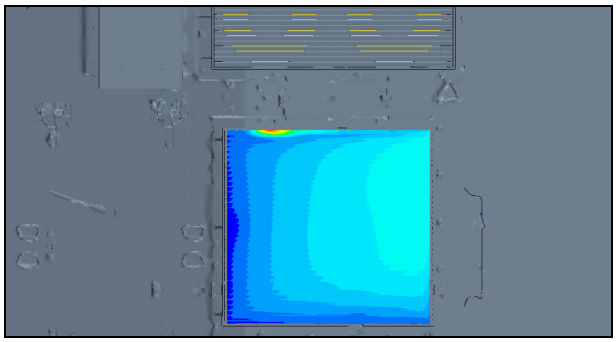

Figure 20: Inlet grille temperatures.

The CFD simulations were also used to predict the system resistance and fan operating point at a given rotation rate. The predicted fan flow volumes and operating points is compared to test data taken using a velocity traverse of at the inlet grille in Figure 21. The comparison is very good for the high rotation rate tests taken at a fan rpm similar to the one simulated.

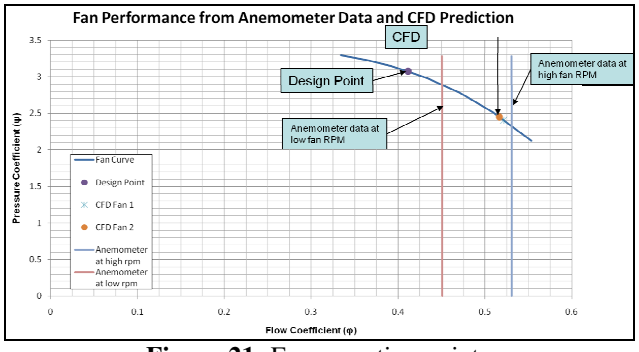

Figure 21: Fan operating points.

When comparing the CFD simulation results to test results for this vehicle, there were some difficulties in determining the air flow rate. A common practice is to calculate the heat rejection from the radiator to the coolant using the coolant flow rate and temperature difference, and then calculate the air flow rate based on the air-side temperature difference across the radiator. In the track vehicle tests there was a large variation in the air temperature measurements taken at both the radiator inlet and outlet. Further investigation showed that some thermocouple readings appeared to be physically unrealistic, making it difficult to accurately determine the air-side temperature difference.

Because of the difficulty in determining the air-side temperature difference, two alternative methods for determining the air flow rate were also employed. Both methods were based on the radiator performance curves obtained from the manufacturer. The first method used the pressure drop measured across the radiator and the pressure versus flow rate curve. The second method was to use the radiator heat transfer versus flow rate curve. A comparison of these two methods and the air-side temperature difference calculation, normalized by the rate calculated using the energy balance method, is shown in Figure 22.

Examining Figure 22 shows that for the majority of the cases the three flow rate calculation methods agree to within 15% of each other. The pressure drop calculation method consistently predicts a higher mass flow rate than the UA method. This is consistent with later test data taken on the radiator core that indicated that the initial pressure drop versus flow rate curve under predicted the pressure drop at higher flow rates.

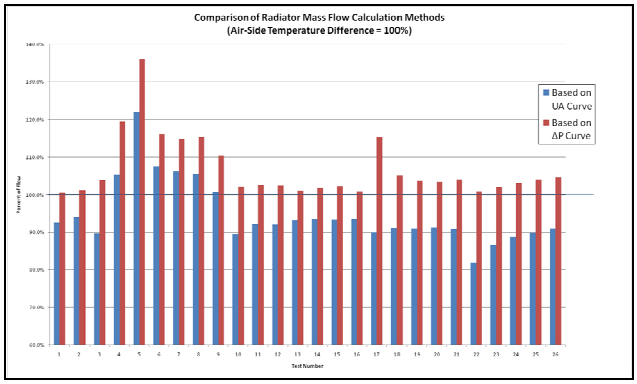

Figure 22: Comparison of air mass flow calculation methods.

CONCLUSIONS AND REMARKS

In general, obtaining fan CAD geometry for use in simulation presents a challenge. Modeling the fan performance using manufacturer data and a momentum source approach appears to give reasonable results for the two vehicles presented in this paper. However, the fan test data is taken under ideal conditions with uniform inlet flow and unobstructed exit flow which rarely exist within an underhood cooling environment. The difference between the fan operating under ideal conditions and in an underhood environment could introduce some error in the predicted vehicle cooling system performance.

Determining the air flow rate based on test data can also be challenging. One method is to use the coolant heat rejection (calculated from the flow rate and radiator top and bottom tank temperature measurements) and air-side temperature difference to determine the mass flow rate of air going through the radiator. It is also important to ensure that both the coolant side and air side temperature measurements are reasonable, because inaccurate temperature readings on either the air or coolant side can have a large effect on the mass flow rate calculation. Alternatively, the heat exchanger maps supplied by the vendor can be used to calculate the air mass flow rate based on the measured heat rejection or air-side pressure drop. Relying on the manufacture data can be problematic because the exchanger performance maps are often calculated for ideal conditions (i.e. uniform velocity and temperature at the heat exchanger inlet). It is advisable to employ each method to ensure that they are reasonably consistent with each other.

For the wheeled MRAP vehicle simulated, the air flow predictions from the simulation agreed well with flow rates calculated using the heat rejection to the coolant and radiator air-side temperature difference, but not with flow rates calculated using the supplier provided radiator heat transfer curves. This was attributed to an over-prediction of the heat transfer characteristics of the radiator in this installation. For the tracked vehicle, the flow rates predicted based on air-side temperature difference, heat exchanger heat transfer curve, and heat exchanger air-side pressure drop agreed fairly well with each other.

For the wheeled MRAP vehicle, the air flow rates predicted in the off-road simulation agreed well with those obtained in the test cell. However, the recirculation patterns observed in the test environment were different than those of the off-road environment. These differences resulted in different air temperatures at the heat exchanger inlet for the two environments. This could lead to an over- or under-prediction of off-road heat exchanger performance.

The elevated inlet grille temperatures observed during testing on the tracked vehicle seemed to indicate that there might be a flow recirculation problem, either due to the layout of the inlet and exit grilles or an interaction with the test chamber. The CFD results showed that recirculation was not likely the cause of the elevated inlet temperatures. Further investigation revealed that temperature stratification at the tunnel inlet was a likely contributor to the increased temperatures.

ACKNOWLEDGEMENTS

The authors would like to acknowledge Dave Ostberg and Paul Maguire from TARDEC for helpful discussions and insights regarding simulation results and John Hubble from TARDEC for providing test results.

REFERENCES

[1] Ross, F., “Vehicle aerodynamics with STAR-CCM+”, presented at STAR Global Transportation Forum 2010, November 9-10, 2010.

[2] Aamodt, S., and Goryca, M., “M109A6 Paladin Self-Propelled Howitzer: Full Load, High Ambient Cooling Test and Follow-on Engineering Tests”, TACOM Research and Development and Engineering Center, Warren, MI, 2004.